Grape seed extract induces anoikis and caspase-mediated apoptosis in human prostate carcinoma LNCaP cells: possible role of ataxia telangiectasia mutated–p53 activation

Manjinder Kaur,[1] Rajesh Agarwal,[1,2] and Chapla Agarwal[1,2]

[1]Department of Pharmaceutical Sciences, School of Pharmacy and [2]University of Colorado Cancer Center, University of Colorado Health Sciences Center, Denver, Colorado

Abstract

Prostate cancer is the second leading cancer diagnosed in elderly males in the Western world. Epidemiologic studies suggest that dietary modifications could be an effective approach in reducing various cancers, including prostate cancer, and accordingly cancer-preventive efficacy of dietary nutrients has gained increased attention in recent years. We have recently shown that grape seed extract (GSE) inhibits growth and induces apoptotic death of advanced human prostate cancer DU145 cells in culture and xenograft. Because prostate cancer is initially an androgen-dependent malignancy, here we used LNCaP human prostate cancer cells as a model to assess GSE efficacy and associated mechanisms. GSE treatment of cells led to their detachment within 12 hours, as occurs in anoikis, and caused a significant decrease in live cells mostly due to their apoptotic death. GSE-induced anoikis and apoptosis were accompanied by a strong decrease in focal adhesion kinase levels, but an increase in caspase-3, caspase-9, and poly(ADP-ribose) polymerase cleavage; however, GSE caused both caspase-dependent and caspase-independent apoptosis as evidenced by cytochrome *c* and apoptosis-inducing factor release into cytosol. Additional studies revealed that GSE causes DNA damage–induced activation of ataxia telangiectasia mutated kinase and Chk2, as well as p53 Ser^{15} phosphorylation and its translocation to mitochondria, suggesting this to be an additional mechanism for apoptosis induction. GSE-induced apoptosis, cell growth inhibition, and cell death were attenuated by pretreatment with *N*-acetylcysteine and involved reactive oxygen species generation. Together, these results show GSE effects in LNCaP cells and suggest additional *in vivo* efficacy studies in prostate cancer animal models. [Mol Cancer Ther 2006;5(5):1265–74]

Introduction

Prostate cancer is the most common cancer occurring in elderly male population in Western countries (1). Contributing risk factors for prostate cancer include age, ethnicity, genetic factors, and diet (2); however, dietary habits are gaining greater importance based on significant findings of various epidemiologic studies, which directly link dietary habits to various forms of cancers, including prostate cancer (3). Thus, identification of bioactive compounds present in diet with potential anticancer efficacy has been an important area of research in recent years for both prevention and intervention of cancers, including prostate cancer (4). Deregulated cell growth and resistance to apoptosis are the major defects in uncontrolled cancer cell growth, suggesting that development of approaches that induce apoptotic machinery within cancer cells could be effective measures against their proliferation and invasive potential (5). In fact, induction of apoptosis in tumor cells is the primary mode of action for most of anticancer therapies, ranging from γ-irradiation, immunotherapy, and chemotherapy (6), and impairment of this pathway is implicated in treatment resistance (7). Apoptosis can be induced either by engagement of death receptors or by stimulation of intrinsic pathway from within the cell in response to variety of stimuli, including withdrawal of growth factors, oncogene activation, DNA damage, etc. (8). Noteworthy here is that many chemopreventive agents of natural origin have shown promising anticancer properties by induction of apoptotic pathway in transformed/tumor cells (9); grape seed extract (GSE) is one such agent.

Over the years, there has been a worldwide interest in GSE as a dietary supplement because of its various health beneficial effects, which are mostly attributed to the high amounts of proanthocyanidins present therein (10). GSE is well tolerated and has been termed as relatively safe in acute, subchronic, and chronic doses in animal studies (11). Recent studies by us and others reveal that GSE exhibits both cancer-preventive and anticancer effects in various animal tumor models and cancer cell lines of different etiologies, such as skin (12), breast (13, 14), colon (15), lung,

Received 1/9/06; revised 3/9/06; accepted 3/24/06.

Grant support: USPHS grant CA91883 awarded by the National Cancer Institute (C. Agarwal).

The costs of publication of this article were defrayed in part by the payment of page charges. This article must therefore be hereby marked advertisement in accordance with 18 U.S.C. Section 1734 solely to indicate this fact.

Requests for reprints: Chapla Agarwal, Department of Pharmaceutical Sciences, School of Pharmacy, University of Colorado Health Sciences Center, 4200 East Ninth Avenue, Box C238, Denver, CO 80262. Phone: 303-315-1382; Fax: 303-315-6281. E-mail: Chapla.Agarwal@uchsc.edu

doi:10.1158/1535-7163.MCT-06-0014

and gastric (16). In case of prostate cancer, studies completed in our laboratory have shown that GSE inhibits the growth of androgen-independent advanced human prostate carcinoma DU145 cells in culture by induction of apoptosis (17), inhibition of constitutive as well as tumor necrosis factor-α–induced nuclear factor-κB activation (18), and by inhibition of epidermal growth factor–induced or constitutive activation of mitogenic signaling (19). Additionally, we have shown that GSE inhibits the growth of DU145 cells as xenograft in nude mice through its *in vivo* antiangiogenic, antiproliferative, and proapoptotic activities (20). Because initial prostate cancer growth is androgen dependent, we assessed GSE efficacy and associated mechanism using hormone-sensitive human prostate carcinoma LNCaP cells as a model system.

Materials and Methods

Reagents

A standardized preparation of GSE was obtained as a gift from its commercial vendor, Kikkoman Corporation (Noda City, Japan). The details of GSE preparation from grape seeds are recently described (11), and the chemical constituents present within this GSE preparation have been analyzed both qualitatively and quantitatively by Yamakoshi et al. (11). They include a total of 89.3% (w/w) procyanidins, a total of 6.6% (w/w) monomeric flavonols, and the remainder includes moisture (2.24%), protein (1.06%), and ash (0.8%; ref. 11). Cleaved caspase-3, caspase-9, cleaved poly(ADP-ribose) polymerase (PARP), focal adhesion kinase (FAK), p53, Ser^{15}-phospho-p53, Ser^{20}-phospho-p53, and Thr^{68}-phospho-Chk2 primary antibodies and peroxidase-conjugated secondary antibodies were from Cell Signaling Technology (Beverly, MA). Ser^{1981}-phospho-ataxia telangiectasia mutated (ATM) antibody was from Rockland Immunochemicals (Gilbertsville, PA). Ser^{139}-phospho-H2A.X antibody was from Upstate (Charlottesville, VA). ATM and apoptosis-inducing factor (AIF) antibodies were from Santa Cruz Biotechnology (Santa Cruz, CA). Cytochrome *c* antibody was from BD PharMingen (San Diego, CA). Hoechst 33342, *N*-acetylcysteine, and propidium iodide (PI) were from Sigma-Aldrich Chemical Co. (St. Louis, MO). Hsp60 antibody was purchased from Stressgen (Victoria, British Columbia, Canada). Annexin V/PI kit was from Molecular Probes (Eugene, OR). Z-VAD.fmk was obtained from Enzyme System Product (Livermore, CA). The enhanced chemiluminescence detection system was from Amersham (Piscataway, NJ). Bio-Rad detergent-compatible protein assay kit was from Bio-Rad Laboratories (Hercules, CA). All other reagents were obtained in their highest purity grade available commercially.

Treatments

Human prostate carcinoma LNCaP cells were obtained from American Type Culture Collection (Manassas, VA). Cells were maintained in RPMI 1640 supplemented with 10% fetal bovine serum and 1% penicillin-streptomycin at 37°C in a humidified 5% CO_2 incubator. GSE was dissolved in DMSO as a thousand-fold concentrated solution and diluted to its final concentration directly into the medium before the culture treatments. Unless specified otherwise, LNCaP cells were plated to 70% confluency for 36 hours and subsequently treated with 10 to 20 μg/mL of GSE up to 24 hours. In Z-VAD.fmk and *N*-acetylcysteine studies, cells were pretreated with Z-VAD.fmk (50 μmol/L for 2 hours) and *N*-acetylcysteine (50 mmol/L for 15 min), respectively, followed by desired GSE treatment.

Cell Growth Viability Assay

LNCaP cells were seeded in 60-mm plates at the density of 5,000 cells/cm^2 and were allowed to grow for 36 hours. Cells were then treated with either DMSO or 10 to 20 μg/mL of GSE for varying time periods. These selections of GSE doses and treatment times are based on an additional study where doses higher than these (e.g., 50 μg/mL GSE) caused complete cell death within 12 hours of treatment (data not shown). At the end of each treatment, nonadherent and adherent cells were collected after brief trypsinization and dead and live cells were counted after trypan blue staining using hemocytometer.

Apoptosis Assays

Quantitative apoptotic cell death by GSE was measured by two independent assays. In first assay using flow cytometric analysis of Annexin V/PI–stained cells, nonadherent and adherent cells were collected subsequent to GSE treatment and were washed twice with PBS. Cells were stained with Annexin V-PI using Vybrant Apoptosis Assay kit 2 essentially as described in the protocol of the manufacturer. In some experiments, the cells were pretreated with Z-VAD.fmk or *N*-acetylcysteine for desired time before treatment with GSE. In the second quantitative apoptotic death assay using Hoechst staining, at the end of GSE treatments, both adherent and nonadherent cells were collected after brief trypsinization. The cells were then stained with DNA-binding dye Hoechst 33342 and PI, and kept on ice until counting was completed. Apoptotic cells were quantified using fluorescent microscope (Axioskope 2 plus-HBO 100, Zeiss, Jena, Germany) by counting 100 cells per microscopic field (at ×100) in five fields in each sample in triplicate.

Immunoblot Analysis

LNCaP cells were grown in RPMI 1640 with 10% fetal bovine serum for 36 hours and then treated with GSE (0–20 μg/mL) for the desired time periods. Total cell lysates, cytosolic fraction, and mitochondrial fraction were then prepared, and protein concentration was determined as recently described (17). For immunoblot analyses, 70 to 100 μg protein per sample was denatured in SDS sample buffer, subjected to SDS-PAGE on 6%, 12%, or 16% Tris-glycine gels, and separated proteins were transferred onto membrane by Western blotting. Membranes were blocked with blocking buffer for 1 hour at room temperature and, as desired, probed with primary antibody against desired molecule overnight at 4°C followed by peroxidase-conjugated appropriate secondary antibody for 1 hour at room temperature and enhanced chemiluminescence detection.

Measurement of Intracellular Reactive Oxygen Species Levels

Intracellular reactive oxygen species (ROS) levels were measured using hROS kit from Cell Technology (Mountain View, CA). Briefly, LNCaP cells were plated at a density of 20,000 cells per well in 24-well cluster plate. Cells were allowed to grow for 36 hours and subsequently loaded with 5 μmol/L APF dye in modified HBSS for 30 minutes in the dark. Cells were then exposed to either GSE (20 μg/mL) or DMSO alone. After 30-minute incubation at 37°C, fluorescence was measured at excitation wavelength of 488 nm and emission wavelength of 515 nm using fluorescence plate reader.

Statistical Analysis

Values were expressed as mean ± SD of three observations. Statistical significance of difference between control and GSE-treated samples was calculated by Student's *t* test using SigmaStat 2.0 (Jandel Scientific, San Rafael, CA). $P < 0.05$ was considered statistically significant. Autoradiograms/bands were scanned with Adobe Photoshop 6.0 (Adobe Systems, Inc., San Jose, CA), and, in each case, blots were subjected to multiple exposures on the film to make sure that the band density is in the linear range. Unless otherwise mentioned, all the data shown in the study are representative of two or three independent experiments.

Results

GSE Inhibits Growth and Induces Death of LNCaP Cells

As shown in Fig. 1A, GSE treatment at the lowest dose did not show any effect up to 24-hour treatment, but caused 20% ($P < 0.05$) decrease in cell growth after 48 hours. Interestingly, 15 μg/mL GSE dose showed 12% to 27% ($P < 0.05$) decrease in cell growth without any time-response effect; however, the highest GSE dose caused a time-dependent effect on cell growth accounting for 39% to 59% ($P < 0.05–0.001$) inhibition (Fig. 1A). In terms of its effect on total live cells only, as shown in Fig. 1B, GSE showed a dose-dependent inhibitory effect; however, a time-response effect was evidenced only for the lowest dose, although higher doses showed strong effect accounting for 30% to 40% ($P < 0.05–0.001$) and 63% to 67% ($P < 0.01–0.001$) inhibition at 15 and 20 μg/mL doses, respectively (Fig. 1B). The other important observation of these cell growth inhibitory effect of GSE was that in all the cases, its inhibitory effect was stronger when considered in terms of a reduction in total live cells (Fig. 1B) versus total cell numbers (Fig. 1A), suggesting a possible cell death effect of the agent. Indeed, based on the trypan blue dye assay results, we also observed a strong cell death effect of GSE. As shown in Fig. 1C, GSE treatment resulted in a strong and a dose-dependent loss of cell viability accounting for 12%, 26%, and 48% ($P < 0.01–0.001$) dead cells at 12 hours of its treatment at 10, 15, and 20 μg/mL doses, respectively. A dose- and a time-response effect of GSE in inducing cell death was also evidenced at 24 hours, but only for 10 and 15 μg/mL doses; a higher GSE dose of 20 μg/mL showed 38% ($P < 0.01–0.001$) cell death that was lower than that observed at 12 hours (Fig. 1C). At 48 hours of treatment, the dead cell population increased from 11% in DMSO control to 22%, 25%, and 25% ($P < 0.05–0.01$) at 10, 15, and 20 μg/mL GSE doses, respectively (Fig. 1C). These results showing that an increase in GSE dose and/or treatment time results in a decrease in its effect on percentage of cell death are in accord with the observation that higher GSE doses and/or treatment times cause a very strong cell death leading to cellular debris that become unaccountable in trypan blue assay.

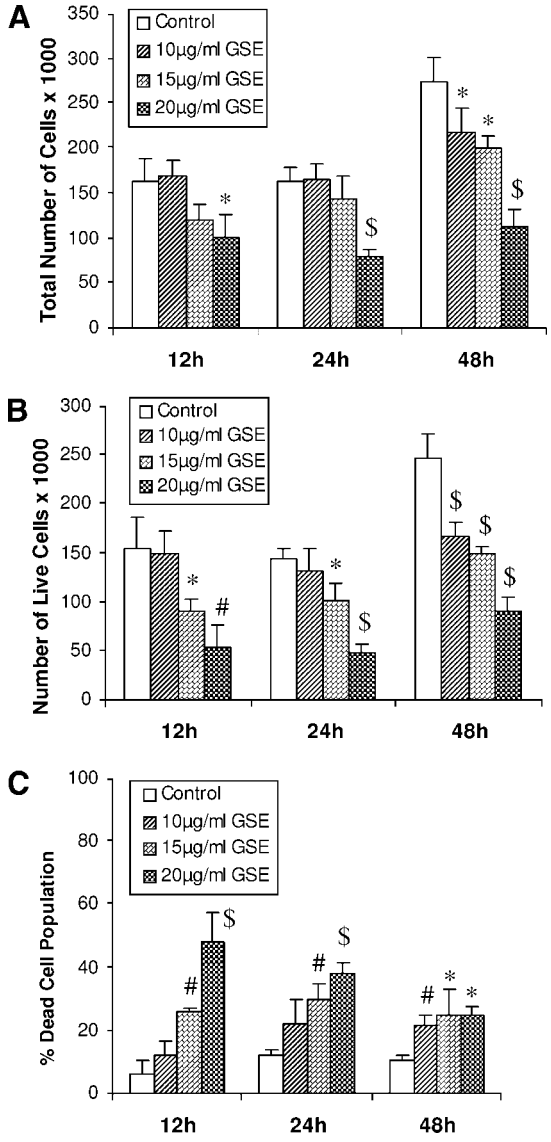

Figure 1. Time- and concentration-dependent growth inhibition and death of LNCaP cells following GSE treatment. LNCaP cells were treated with GSE (0–20 μg/mL) for 12 to 48 h, and adherent as well as nonadherent cells were collected after respective treatment time and counted on hemocytometer after trypan blue staining for total number of cell (**A**), total number of live cells (**B**), and percentage of dead cell population (**C**). *Columns*, mean of three values; *bars*, SD. *, $P < 0.05$; #, $P < 0.01$; $, $P < 0.001$, statistical significance in GSE-treated groups compared with DMSO controls.

GSE Causes Anoikis in LNCaP Cells and Decreases FAK Levels

During the entire cell growth and viability assay, we also examined the cultures under microscope for any possible changes in cell morphology following GSE treatments. We observed that GSE treatment of cells makes them rounded followed by their detachment from the plastic (Fig. 2A). This effect was strongest at 20 μg/mL GSE dose and occurred as early as 5 to 6 hours posttreatment time where all the cells became rounded and got detached from tissue culture dish (Fig. 2A), suggesting that GSE might be causing anoikis-like apoptotic cell death by possibly reducing the cellular adhesion to extracellular matrix by altering FAK levels (21). Accordingly, we next assessed the level of FAK in 20 μg/mL GSE-treated LNCaP cells as a function of early time points starting with 30 minutes. As shown in Fig. 2B, this dose of GSE, which showed complete cell rounding and detachment from the plastic within 5 to 6 hours, also showed a time-dependent decrease in FAK protein level. The GSE effect on FAK decrease was evidenced as early as 1 hour, which became more prominent at 2 hours. By 6 to 12 hours, almost all the FAK protein level diminished in GSE-treated cells (Fig. 2B).

GSE Causes Apoptotic Death of LNCaP Cells

Based on the results showing that GSE causes a strong death of LNCaP cells together with its anoikis effect, next studies were done to assess whether this was an apoptotic cell death. Experiments, however, were done only up to 24 hours because longer GSE treatment caused very strong cell death that also results in cell debris. As shown in Fig. 3A, using Annexin V/PI staining and fluorescence-activated cell sorting analysis, we observed that GSE causes a strong dose-dependent apoptotic death of LNCaP cells. Compared with DMSO control showing 15% apoptotic cells, GSE treatment of cells at 10, 15, and 20 μg/mL doses for 12 hours resulted in 18%, 33%, and 67% ($P < 0.01–0.001$) apoptotic cell population accounting for ~1.2- to 4.5-fold increase over control, respectively (Fig. 3A). No additional apoptotic effect of GSE was observed following LNCaP cell treatment at similar dose levels for 24 hours except at

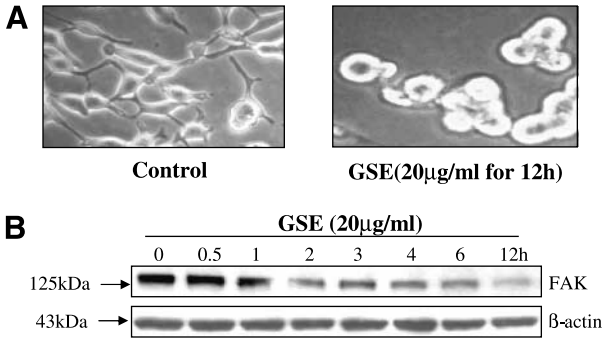

Figure 2. GSE causes anoikis and decreases FAK levels in LNCaP cells. **A,** cells were treated with GSE (20 μg/mL) for 12 h and cell morphology was examined under a light microscope. Magnification, ×200. **B,** Western blot analysis was done to determine FAK levels. Actin was used as a loading control.

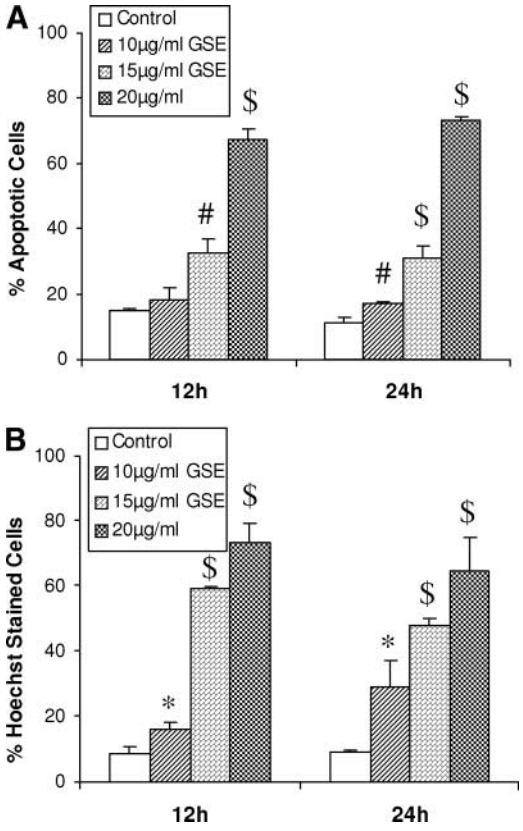

Figure 3. GSE causes apoptotic death of LNCaP cells. Cells were treated with GSE (0 – 20 μg/mL) for different time intervals (0 – 24 h), and adherent and nonadherent cells were collected and stained with Annexin V-PI or Hoechst. The percentage of apoptotic cell death was measured by FACScan analysis of Annexin V-PI – stained cells (**A**), and manual counting of Hoechst-stained cells (**B**). *Columns*, mean of three values; *bars*, SD. *, $P < 0.05$; #, $P < 0.01$; $, $P < 0.001$, statistical significance in GSE-treated groups compared with DMSO controls.

20 μg/mL dose showing 73% ($P < 0.001$) apoptotic cell population (Fig. 3A). We also determined the extent of apoptosis after GSE treatment in LNCaP cells by Hoechst staining. As shown in Fig. 3B, compared with DMSO-treated control cells showing 8.5% Hoechst-stained cells, GSE treatment at 10, 15, and 20 μg/mL doses for 12 hours resulted in a strong and dose-dependent increase in Hoechst-stained cells (16%, 59%, and 74%, $P < 0.05–0.001$) accounting for an ~2- to 9-fold increase over control. Similar results were also observed following GSE treatment at these doses for 24 hours (Fig. 3B). Together, the data obtained using two different assays clearly show a strong apoptotic effect of GSE in LNCaP cells (Fig. 3). It is to be noted here that extent of apoptotic cell death observed with these assays following GSE treatment is higher than the extent of cell death observed with trypan blue exclusion assay. This may possibly be due to the fact that Annexin V/PI and Hoechst staining are much more sensitive assays capable of accounting cells undergoing both early and late apoptotic death, whereas trypan blue stains the cells when they are completely dead.

To assess whether the observed biological effects of GSE in Figs. 1 to 3 are specific and not due to change in the pH of culture medium in the presence of GSE, cells were also treated with sodium citrate at 20 μg/mL dose and medium pH was also determined following GSE addition. Sodium citrate did not show any effect as GSE, and medium pH did not change with GSE, suggesting that GSE effects observed are specific and are not due to change in medium pH (data not shown).

GSE-Caused Apoptosis Involves Caspase-9, Caspase-3, and PARP Cleavage

Activation of both extrinsic and intrinsic caspase pathways has been well established to be the major mechanisms of apoptotic cell death in most cellular systems (22). Based on our findings showing that GSE causes a strong apoptotic death of LNCaP cells, we first assessed whether GSE activates caspase pathways. Treatment of cells with GSE did not result in caspase-8 activation and cleavage (data not shown); however, it caused a strong dose- and time-dependent cleavage of caspase-9, caspase-3, and PARP (Fig. 4A). Because we observed maximum apoptotic cell death and its associated cleavage of caspases and PARP at 20 μg/mL GSE dose as early as 12 hours of treatment, we selected this GSE dose level to study the time kinetics of molecular events involved in GSE-induced apoptosis. As shown in Fig. 4B, GSE treatment of LNCaP cells at this dose resulted in caspase-9 and its downstream caspase-3 cleavage as early as 3 hours with an increase at later time points, although maximum effect was evidenced at 12 hours. The observed cleavage of caspase-9 and caspase-3 was accompanied with a comparable time kinetics for PARP cleavage (Fig. 4B).

GSE-Caused Apoptosis Involves Cytochrome *c* and AIF Release into Cytosol, and Occurs via Both Caspase-Dependent and Caspase-Independent Pathways

The observed activation of caspase-9 without an effect on caspase-8 by GSE suggested an involvement of intrinsic pathway of apoptosis. As one of the hallmarks of intrinsic pathway of apoptosis is the release of mitochondrial cytochrome *c* into the cytosol (8, 23), we next assessed whether GSE treatment of cells also results in mitochondrial release of cytochrome *c* into the cytosol. Under similar conditions as for other studies, treatment of LNCaP cells with GSE (20 μg/mL) resulted in a time-dependent release of cytochrome *c* into the cytosol (Fig. 4C). Altogether, the data shown in Fig. 4A to C clearly indicate that GSE activates intrinsic caspase cascade via cytochrome *c* release into the cytosol from the mitochondria, leading to caspase-9 followed by caspse-3 activation that results in PARP cleavage and apoptotic cell death. To further support this suggestion and establish that indeed this is the only mechanism of GSE-induced apoptotic death of LNCaP cells, we next pretreated the cells with pan-caspase inhibitor Z-VAD.fmk for 2 hours followed by GSE treatment at 20 μg/mL dose for 12 hours. The extent of apoptosis was then determined by Annexin V-PI staining and fluorescence-activated cell sorting analysis. In this experiment, we observed that Z-VAD.fmk pretreatment reversed GSE-induced apoptosis only by 23% ($P < 0.01$); although this reversal is statistically significant, it suggests that caspase-independent mechanisms are also involved in GSE-induced apoptotic cell death (Fig. 4D) at least under caspase-inhibiting conditions. Several mechanisms of caspase-independent apoptotic cell death have been reported in recent years, out of which release of AIF that normally resides within mitochondria is often implicated in caspase-independent apoptosis (24). Accordingly, we first assessed whether GSE causes AIF release from the mitochondria. Under identical treatments as for other studies, GSE treatment of LNCaP cells led to a time-dependent release of AIF from the mitochondria as evidenced by its strong levels in cytosolic fractions from GSE-treated cells compared with almost no detectable levels in DMSO controls (Fig. 4C).

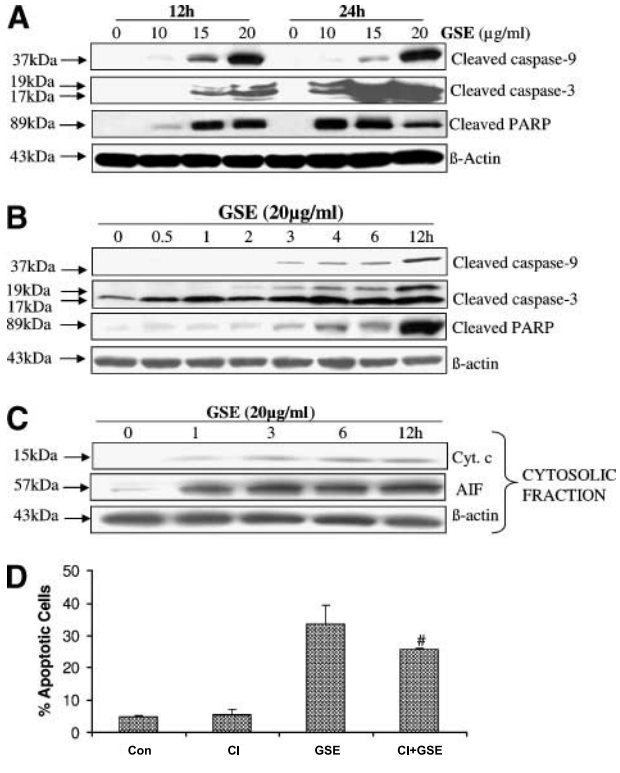

Figure 4. GSE induces caspase-dependent and caspase-independent pathways of apoptosis. **A,** LNCaP cells were treated with GSE (0–20 μg/mL) for 12 and 24 h, and Western blot analysis was done for cleaved caspase-9, caspase-3, and PARP. **B,** time kinetics of caspase-9, caspase-3, and PARP cleavage following GSE (20 μg/mL) treatment of LNCaP cells for 0 to 12 h. **C,** time kinetics of release of cytochrome *c* and AIF into cytosol following GSE (20 μg/mL) treatment of LNCaP cells. **D,** LNCaP cells pretreated with or without z-VAD.fmk (*CI*, 50 μmol/L, 2 h) were incubated with DMSO (control, *Con*) or GSE (20 μg/mL) for another 12 h. Adherent and nonadherent cells were collected after brief trypsinization and were stained with Annexin V/PI. Extent of apoptosis was assessed by fluorescence-activated cell sorting analysis of stained cells. *Columns*, mean of three values; *bars*, SD; #, $P < 0.01$, statistical significance in Z-VAD.fmk + GSE–treated group compared with GSE-alone group.

GSE Causes Ser^{139} Phosphorylation of Histone H2A.X in LNCaP Cells

Several studies in recent years have shown that various cancer chemopreventive agents also induce apoptotic death of cancer cells by DNA-damaging mechanisms (25, 26). In response to DNA damage, phosphorylation of histone H2A.X is the earliest cellular event marked by the presence of visible foci in damaged cells (27). Because we observed that GSE causes a substantial apoptotic cell death by a caspase-independent mechanism, specifically under caspase-inhibiting conditions, we next assessed whether GSE causes DNA damage that is responsible for its additional apoptotic mechanism. Treatment of LNCaP cells with GSE at 20 μg/mL dose resulted in DNA damage as evidenced by an appearance of Ser^{139} phosphorylated histone H2A.X in GSE-treated cells in immunoblot analysis (Fig. 5A). A time kinetics study of GSE-treated cells showed Ser^{139} phosphorylated H2A.X band after 4 hours of treatment, which became stronger at 6 hours followed by 12 hours (Fig. 5A). Immunocytochemical staining of GSE-treated cells also showed Ser^{139}-phosphorylated histone H2A.X foci (data not shown).

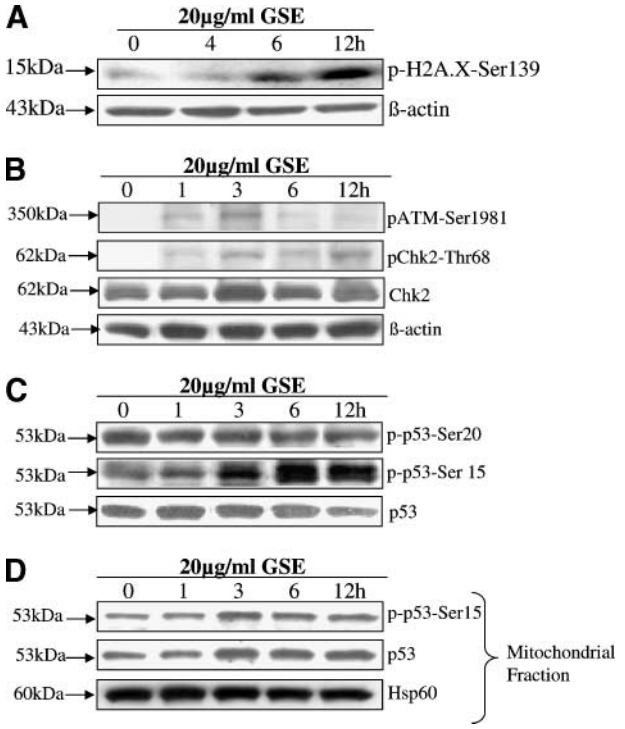

Figure 5. GSE causes Ser^{139} phosphorylation of histone H2A.X, ATM-Chk2 activation, and p53 phosphorylation at Ser^{15} and mitochondrial translocation in LNCaP cells. LNCaP cells were treated with GSE (20 μg/mL) for the indicated time, and Western blot analysis was done in total cell lysates to determine phosphorylated H2A.X (**A**), phosphorylated and total levels of ATM and Chk2 (**B**), and phosphorylated and total levels of p53 (**C**). **D,** phosphorylated and total levels of p53 were analyzed by Western blotting in mitochondrial fractions.

GSE Causes ATM-Chk2 Activation and p53 Phosphorylation at Ser^{15} and Mitochondrial Translocation in LNCaP Cells

DNA damage is known to activate phosphatidylinositol 3-kinase family of kinases, including ATM, ATR, and DNA-PK (28). Among them, however, in recent years, ATM is well studied and is established as a major player to be activated by cancer-chemopreventive agents following their DNA-damaging activity (26). ATM activation then leads to Chk-p53 activation followed by an apoptotic death (26, 29, 30). Based on the observation that GSE causes Ser^{139} phosphorylation of H2A.X, we next assessed whether this effect of GSE is also associated with ATM-Chk-p53 activation. As shown in Fig. 5B, treatment of LNCaP cells with GSE resulted in Ser^{1981} phosphorylation of ATM as early as 1 hour, which became very strong after 3 hours and then started decreasing. In terms of Chk phosphorylation, no effect of GSE was observed on Chk1; however, immunoblot analysis for total and Thr^{68}-phosphorylated Chk2 revealed increased Thr^{68} phosphorylation of Chk2 over control, occurring as early as 1 hour after GSE treatment. Phosphorylation persisted until the end of the experiment duration of 12 hours without any change in total Chk2 levels (Fig. 5B). As p53 is known to get activated and/or stabilized depending on its phosphorylation at multiple sites by a number of kinases, including ATM-Chk activation in response to DNA damage (31, 32), we next examined the phosphorylation of p53 at two key residues, Ser^{15} and Ser^{20}. Using phosphorylation site–specific antibodies for p53, we found that GSE causes the phosphorylation of p53 at Ser^{15} without affecting the phosphorylation at Ser^{20} residue as well as total p53 levels (Fig. 5C). Phosphorylation of p53 at Ser^{20} residue is generally associated with its stability, whereas phosphorylation at Ser^{15} is associated with its apoptosis-inducing effect (33). We therefore also examined whether p53 translocates to mitochondria subsequent to GSE treatment. Western blot analysis with antibody for total p53 revealed that there was a time-dependent increase in translocation of p53 to mitochondria (Fig. 5D), and that with phosphospecific p53 antibody revealed that translocated p53 was Ser^{15}-phosphorylated form (Fig. 5D).

GSE-Induced Biological Effects in LNCaP Cells Are Attenuated by Pretreatment with *N*-Acetylcysteine and Involve ROS Production

In the present study, we observed that GSE treatment of cells results in DNA damage and associated activation of ATM-Chk2-p53, a pathway that is normally activated by various prooxidant stimuli, such as ionizing radiation, hyperoxia, etc. (29, 30). Furthermore, several studies in recent years have shown that various cancer-chemopreventive agents activate ATM-Chk-p53 pathway followed by apoptotic death of the cancer cells via an oxidative mechanism (25). Together, based on our own observations and those reported in literature, we next studied whether GSE causes oxidative stress that is responsible for its apoptotic effect. Pretreatment of LNCaP cells with 50 mmol/L

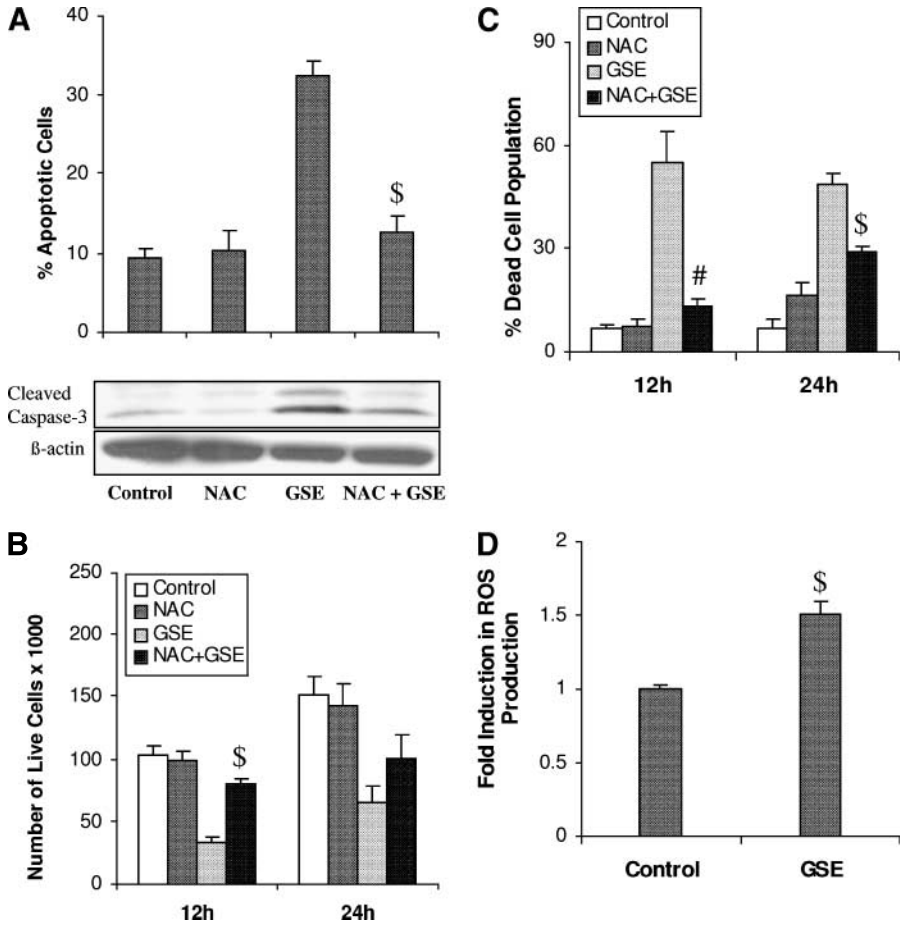

Figure 6. GSE-induced biological effects in LNCaP cells are attenuated by pretreatment with *N*-acetylcysteine and involve ROS production. LNCaP cells were pretreated with 50 mmol/L *N*-acetylcysteine (*NAC*) followed by treatment with GSE (20 μg/mL) for 4 h. **A,** adherent and nonadherent cells were collected thereafter by brief trypsinization and stained with Annexin-V/PI to quantify apoptotic cell death by fluorescence-activated cell sorting analysis. Representative of two independent experiments with identical findings. In addition, Western blot analysis was done to determine the caspase-3 cleavage following indicated treatments. Number of live cells (**B**) and percentage of dead cell population (**C**) were measured by counting the cells on the hemocytometer after trypan blue staining, after pretreatment of LNCaP cells with 50 mmol/L *N*-acetylcysteine followed by treatment with GSE (20 μg/mL) for 12 and 24 h. **D,** intracellular ROS production was measured following protocol provided with hROS kit by measuring fluorescence using fluorescence plate reader. *Columns*, mean of three values; *bars*, SD. #, $P < 0.01$; $, $P < 0.001$, statistical significance in *N*-acetylcysteine + GSE–treated group compared with GSE alone.

N-acetylcysteine for 15 minutes before GSE (20 μg/mL) treatment resulted in a significant reversal (60%, $P < 0.001$) of GSE-caused apoptosis (Fig. 6A), which was also in accord with a marked reduction in GSE-caused cleaved caspase-3 by *N*-acetylcysteine pretreatment of the cells under identical experimental conditions (Fig. 6A). Additionally, we observed that *N*-acetylcysteine pretreatment of LNCaP cells before GSE treatment for 12 hours led to a significant increase in the total live cell population (76%, $P < 0.001$) compared with that observed with GSE alone (32%; Fig. 6B). However, this effect with *N*-acetylcysteine pretreatment became statistically insignificant after 24 hours of treatment with GSE. In case of percentage of dead cells, under similar treatment conditions, 76% ($P < 0.01$) and 40% ($P < 0.001$) reversal was observed following *N*-acetylcysteine pretreatment at 12 and 24 hours of GSE treatment (Fig. 6C). Based on these results, it was pertinent to also measure the extent of intracellular ROS generation by GSE, if any. Using ROS-sensitive fluorescent probe, we found that treatment of LNCaP cells with GSE (20 μg/mL) results in ~1.5-fold induction in ROS production compared with DMSO-treated control. Together, these results suggest that GSE-induced apoptosis is also mediated through generation of ROS, which, in turn, possibly activates both intrinsic pathway of apoptosis as well as the one via ATM-p53. More studies in the future, however, are needed to support these suggestions.

Discussion

Chemoprevention of prostate cancer holds a great promise due to a long latency period between premalignant lesion known as prostatic intraepithelial neoplasia and clinically proven form of malignancy (34). In this regard, chemopreventive agents, which are of natural origin and often a part of diet daily consumed by a person, provide a less expensive and an effective alternative for controlling the outcome of this disease. Vegetables and fruits are excellent sources of such chemopreventive agents as at least 35 different plant-based foods have been identified by the National Cancer Institute to be effective in the prevention of cancer (9). These agents, initially classified into two broad categories, namely blocking agents and suppressing agents, have now been recognized to impinge upon various molecular targets, thereby limiting the use of old classification (9). A wide range of studies in recent years have convincingly shown that these agents affect the process of

carcinogenesis by regulating pathways ranging from carcinogen activation, detoxification, DNA repair, cell cycle progression, and differentiation to induction of apoptosis in transformed cells.

In the present study, we studied the efficacy of GSE against prostate cancer using LNCaP cells as a model for androgen-dependent initial stage of this malignancy. We observed that GSE causes both anoikis and apoptosis involving FAK level decrease, but a strong caspase and PARP cleavage. GSE treatment of cells also released cytochrome *c* from the mitochondria to the cytosol, suggesting an activation of intrinsic pathway of apoptosis; however, the pan-caspase inhibitor Z-VAD.fmk failed to completely attenuate GSE-induced apoptosis, implying that caspase-independent pathways are also involved in GSE-induced apoptosis. Numerous studies have examined the involvement of caspase independent mechanisms of apoptosis and have implicated various noncysteine proteases, such as serine proteases, granzyme A, calpains, and AIF, in this form of cell death (35, 36). Of these noncysteine proteases, AIF is thought to mediate apoptosis through caspase-independent pathway, where following a death stimulus mitochondrial AIF is released into cytosol, which then translocates to nucleus and causes nuclear condensation followed by massive chromatin fragmentation and cell death (37, 38). In our study, we found that GSE treatment of LNCaP cells lead to release of AIF from mitochondria, which was in accord with the involvement of both caspase-dependent and caspase-independent pathways of apoptosis induction by GSE.

An apoptosis induction also occurs in response to varied types of death stimuli ranging from growth/survival factor deprivation, endoplasmic reticulum stress agents, replication stress, free radicals/oxidative stress, metabolic poisons, and oncogene activation to DNA damage (39). With regard to DNA damage–caused apoptotic cell death, one of the markers of DNA double-strand breaks is the phosphorylation of H2A.X at Ser^{139} (27). In our study, we found that GSE causes DNA damage as evidenced by phosphorylation of H2A.X at Ser^{139} as a function of time after GSE treatment. It is important to emphasize here that hyperphosphorylation of H2A.X strongly correlates to apoptotic chromatin fragmentation (40), suggesting that GSE causes DNA damage and associated apoptotic death of LNCaP cells.

In response to DNA damage, a tumor suppressor protein p53 is stabilized and activated as a transcription factor, primarily by posttranscriptional mechanisms (31, 32). DNA damage induces multiple p53 posttranslational modifications, including phosphorylation at multiple sites, such as Ser^{6}, Ser^{9}, Ser^{15}, Ser^{20}, Ser^{37}, and Ser^{392}; dephosphorylation at Ser^{376}; and acetylation of Lys^{320}, Lys^{373}, and Lys^{382} (41). In our study, we found that p53 was phosphorylated at Ser^{15} subsequent to GSE treatment; however, the steady-state levels of total p53 remained unaltered and there was no increase in p53 phosphorylation at Ser^{20} residue, suggesting that Ser^{15} phosphorylation of p53 might be responsible for the apoptotic effect of GSE. This suggestion is in agreement with recent studies where phosphorylation of Ser^{15} has been found to be critical for apoptotic activity of p53 (33).

Phosphorylation of p53 in response to DNA damage could occur by various kinases, such as ATM, ATR, and DNA-PK; however, ATM and ATR phosphorylate p53 only at the Ser^{15} residue (42). In our study, ATM activation was observed upon GSE treatment of LNCaP cells as evidenced by its phosphorylation at Ser^{1981}, which might be responsible for p53 phosphorylation at Ser^{15} without an effect on Ser^{20} phosphorylation. Following DNA damage, an autophosphorylation of ATM at Ser^{1981} is required for the activation of ATM, which then phosphorylates downstream targets such as Chk2, p53, and H2A.X (43). Indeed, all these downstream targets of activated ATM were found to be phosphorylated in our study following GSE treatment of LNCaP cells. In a study by Hammond et al. (44), ATM activity was observed to increase in response to the oxidative stress of reoxygenation, and even the downstream targets of ATM, such as H2A.X and p53, were also phosphorylated under similar conditions, suggesting the involvement of ROS in DNA damage–induced activation of damage response pathway. In our study, we also found that GSE-induced apoptosis, cell growth inhibition, and cell death were attenuated by pretreatment with *N*-acetylcysteine, suggesting the involvement of ROS in its apoptotic activity that might be a consequence of oxidative stress–caused DNA damage. Whereas this suggestion is contrary to the fact that GSE, being a rich source of proanthocyanidins, is expected to be a scavenger of ROS due to its antioxidant activity, there are reports in literature showing that plant phenolics also act as prooxidants under certain conditions (45). In fact, it has been shown recently that depending on its concentration, GSE itself could lead to the production of hydrogen peroxide (46). Consistent with these reports and our *N*-acetylcysteine results, we did find an increase in ROS production in GSE-treated cells.

Several mechanisms of apoptosis induction by p53 have been identified involving transcriptional and/or nontranscriptional regulation of its downstream effectors (47). For example, p53 is known to induce apoptosis by transcriptional up-regulation of proapoptotic genes such as *Noxa*, *Puma*, *Bax*, *Apaf-1*, *AIP*, and by transcriptional repression of Bcl2 and inhibitors of apoptosis (47). However, in our study, we found that GSE treatment does not alter the levels of Bcl2 and Bax (data not shown). In case of nontranscriptional mechanisms, it has been found that p53 translocates to mitochondria preceding cytochrome *c* release and pro-caspase-3 activation (48). It has also been reported that p53 induces apoptosis via physical interaction with the antiapoptotic proteins Bcl2 and Bcl-XL through its DNA-binding domain, thus leading to sequestration of these proteins from their interaction with proapoptotic partners, Bax/Bak proteins, and, as a result, Bax/Bak can form oligomers and permeabilize the outer mitochondrial membrane, thereby causing the release of mitochondrial

cytochrome *c* to cytosolic compartment of the cell (49). Further, it has been recently shown that Eugenol, a principal component of *Szygium aromaticum* (L.) Merr. Et Perry flower bud (cloves), induces apoptosis in mast cells by translocation of Ser^{15} phospho-p53 into the mitochondria where it interacts with Bcl-2 and Bcl-XL, thus abrogating their survival function (50). Consistent in part with these studies, we also observed the translocation of Ser^{15} phospho-p53 to the mitochondria in GSE-treated cells, which might be responsible in inducing apoptotic death of LNCaP cells by similar mechanisms. Additional studies, however, are required in the future to further elucidate the exact mechanism and role of Ser^{15} phospho-p53 translocation to mitochondria in GSE-induced apoptotic cell death.

References

1. Jemal A, Murray T, Ward E, et al. Cancer statistics, 2005. CA Cancer J Clin 2005;55:10 – 30.
2. Crawford ED. Epidemiology of prostate cancer. Urology 2003;62: 3 – 12.
3. Bidoli E, Talamini R, Bosetti C, et al. Macronutrients, fatty acids, cholesterol and prostate cancer risk. Ann Oncol 2005;6:152 – 7.
4. Kelloff GJ, Crowell JA, Steele VE, et al. Progress in cancer chemoprevention. Ann N Y Acad Sci 1999;889:1 – 13.
5. Denmeade SR, Isaacs JT. Programmed cell death (apoptosis) and cancer chemotherapy. Cancer Control 1996;3:303 – 9.
6. Lake RA, Robinson BW. Immunotherapy and chemotherapy—a practical partnership. Nat Rev Cancer 2005;5:397 – 405.
7. Johnstone RW, Ruefli AA, Lowe SW. Apoptosis: a link between cancer genetics and chemotherapy. Cell 2002;108:153 – 64.
8. Riedl SJ, Shi Y. Molecular mechanisms of caspase regulation during apoptosis. Nat Rev Mol Cell 2004;11:897 – 907.
9. Surh YJ. Cancer chemoprevention with dietary phytochemicals. Nat Rev Cancer 2003;3:768 – 80.
10. Bagchi D, Bagchi M, Stohs SJ, et al. Free radicals and grape seed proanthocyanidin extract: importance in human health and disease prevention. Toxicology 2000;148:187 – 97.
11. Yamakoshi J, Saito M, Kataoka S, Kikuchi M. 2002 Safety evaluation of proanthocyanidin-rich extract from grape seeds. Food Chem Toxicol 2004;40:599 – 607.
12. Zhao J, Wang J, Chen Y, Agarwal R. Anti-tumor-promoting activity of a polyphenolic fraction isolated from grape seeds in the mouse skin two-stage initiation-promotion protocol and identification of procyanidin B5-3′-gallate as the most effective antioxidant constituent. Carcinogenesis 1999;20:1737 – 45.
13. Sharma G, Tyagi AK, Singh RP, Chan DC, Agarwal R. Synergistic anticancer effects of grape seed extract and conventional cytotoxic agent doxorubicin against human breast carcinoma cells. Breast Cancer Res Treat 2004;85:1 – 12.
14. Eng ET, Ye J, Williams D, et al. Suppression of estrogen biosynthesis by procyanidin dimers in red wine and grape seeds. Cancer Res 2003;63: 8516 – 22.
15. Durak I, Cetin R, Devrim E, Erguder IB. Effects of black grape extract on activities of DNA turn-over enzymes in cancerous and non cancerous human colon tissues. Life Sci 2005;76:2995 – 3000.
16. Ye X, Krohn RL, Liu W, et al. The cytotoxic effects of a novel IH636 grape seed proanthocyanidin extract on cultured human cancer cells. Mol Cell Biochem 1999;196:99 – 108.
17. Agarwal C, Singh RP, Agarwal R. Grape seed extract induces apoptotic death of human prostate carcinoma DU145 cells via caspases activation accompanied by dissipation of mitochondrial membrane potential and cytochrome *c* release. Carcinogenesis 2002;23:869 – 76.
18. Dhanalakshmi S, Agarwal R, Agarwal C. Inhibition of NF-κB pathway in grape seed extract-induced apoptotic death of human prostate carcinoma DU145 cells. Int J Oncol 2003;23:721 – 7.
19. Tyagi A, Agarwal R, Agarwal C. Grape seed extract inhibits EGF-induced and constitutively active mitogenic signaling but activates JNK in human prostate carcinoma DU145 cells: possible role in antiproliferation and apoptosis. Oncogene 2003;22:1302 – 16.
20. Singh RP, Tyagi AK, Dhanalakshmi S, Agarwal R, Agarwal C. Grape seed extract inhibits advanced human prostate tumor growth and angiogenesis and up-regulates insulin-like growth factor binding protein-3. Int J Cancer 2004;108:733 – 40.
21. Kabir J, Lobo M, Zachary I. Staurosporine induces endothelial cell apoptosis via focal adhesion kinase dephosphorylation and focal adhesion disassembly independent of focal adhesion kinase proteolysis. Biochem J 2002;367:145 – 55.
22. Fadeel B, Orrenius S. Apoptosis: a basic biological phenomenon with wide-ranging implications in human disease. J Intern Med 2005;258: 479 – 517.
23. Jiang X, Wang X. Cytochrome *c*-mediated apoptosis. Annu Rev Biochem 2004;73:87 – 106.
24. Dawson VL, Dawson TM. Deadly conversations: nuclear-mitochondrial cross-talk. J Bioenerg Biomembr 2004;36:287 – 94.
25. Singh SV, Herman-Antosiewicz A, Singh AV, et al. Sulforaphane-induced G_2/M phase cell cycle arrest involves checkpoint kinase 2-mediated phosphorylation of cell division cycle 25C. J Biol Chem 2004; 279:25813 – 22.
26. Ye R, Bodero A, Zhou BB, Khanna KK, Lavin MF, Lees-Miller SP. The plant isoflavenoid genistein activates p53 and Chk2 in an ATM-dependent manner. J Biol Chem 2001;276:4828 – 33.
27. Rogakou EP, Pilch DR, Orr AH, Ivanova VS, Bonner WM. DNA Double-stranded breaks induce histone H2AX phosphorylation on serine 139. J Biol Chem 1998;273:5858 – 68.
28. Abraham RT. PI 3-kinase related kinases: ''big'' players in stress-induced signaling pathways. DNA Repair (Amst) 2004;3:883 – 7.
29. Kurz EU, Douglas P, Lees-Miller SP. Doxorubicin activates ATM-dependent phosphorylation of multiple downstream targets in part through the generation of reactive oxygen species. J Biol Chem 2004;279: 53272 – 81.
30. Helt CE, Cliby WA, Keng PC, Bambara RA, O'Reilly MA. Ataxia telangiectasia mutated (ATM) and ATR and Rad3-related protein exhibit selective target specificities in response to different forms of DNA damage. J Biol Chem 2005;280:1186 – 92.
31. Ashcroft M, Vousden KH. Regulation of p53 stability. Oncogene 1999;18:7637 – 43.
32. Kastan MB, Onyekwere O, Sidransky D, Vogelstein B, Craig RW. Participation of p53 protein in the cellular response to DNA damage. Cancer Res 1991;51:6304 – 11.
33. Chehab NH, Malikzay A, Stavridi ES, Halazonetis TD. Phosphorylation of Ser-20 mediates stabilization of human p53 in response to DNA damage. Proc Natl Acad Sci U S A 1999;96:13777 – 82.
34. Klein EA. Chemoprevention of prostate cancer. Crit Rev Oncol Hematol 2005;54:1 – 10.
35. Eeva J, Pelkonen J. Mechanisms of B cell receptor induced apoptosis. Apoptosis 2004;9:525 – 31.
36. Martinvalet D, Zhu P, Lieberman J. Granzyme A induces caspase-independent mitochondrial damage, a required first step for apoptosis. Immunity 2005;22:355 – 70.
37. Susin SA, Lorenzo HK, Zamzami N, et al. Molecular characterization of mitochondrial apoptosis-inducing factor. Nature 1999;397:441 – 6.
38. Joza N, Susin SA, Daugas E, et al. Essential role of the mitochondrial apoptosis-inducing factor in programmed cell death. Nature 2001;410: 549 – 54.
39. Fumarola C, Guidotti GG. Stress-induced apoptosis: toward a symmetry with receptor-mediated cell death. Apoptosis 2004;9:77 – 82.
40. Talasz H, Helliger W, Sarg B, Debbage PL, Puschendorf B, Lindner H. Hyperphosphorylation of histone H2A.X and dephosphorylation of histone H1 subtypes in the course of apoptosis. Cell Death Differ 2002;9:27 – 39.
41. Xu Y. Regulation of p53 responses by post-translational modifications. Cell Death Differ 2003;10:400 – 3.
42. Shieh SY, Ikeda M, Taya Y, Prives C. DNA damage-induced phosphorylation of p53 alleviates inhibition by MDM2. Cell 1997;91: 325 – 34.
43. Bakkenist CJ, Kastan MB. DNA damage activates ATM through

intermolecular autophosphorylation and dimmer dissociation. Nature 2003;421:499 – 506.

44. Hammond EM, Giaccia AJ. The role of ATM and ATR in the cellular response to hypoxia and re-oxygenation. DNA Repair (Amst) 2004;3: 1117 – 22.

45. Hadi SM, Asad SF, Singh S, Ahmad A. Putative mechanism for anticancer and apoptosis-inducing properties of plant-derived polyphenolic compounds. IUBMB Life 2000;50:167 – 71.

46. Sugisawa A, Inoue S, Umegaki K. Grape seed extract prevents H(2)O(2)-induced chromosomal damage in human lymphoblastoid cells. Biol Pharm Bull 2004;27:1459 – 61.

47. Yee KS, Vousden KH. Complicating the complexity of p53. Carcinogenesis 2005;26:1317 – 22.

48. Marchenko ND, Zaika A, Moll UM. Death signal-induced localization of p53 protein to mitochondria. A potential role in apoptotic signaling. J Biol Chem 2000;275:16202 – 12.

49. Scorrano L, Korsmeyer SJ. Mechanisms of cytochrome *c* release by proapoptotic BCL-2 family members. Biochem Biophys Res Commun 2003;304:437 – 44.

50. Park BS, Song YS, Yee SB, et al. Phospho-ser 15-p53 translocates into mitochondria and interacts with Bcl-2 and Bcl-xL in eugenol-induced apoptosis. Apoptosis 2005;10:193 – 200.